

Covariant model for proton-proton bremsstrahlung: comparison with high-precision data

M.D. Cozma,^a G.H. Martinus,^a O. Scholten,^a

R.G.E. Timmermans,^a J.A. Tjon^{a,b}

^a *KVI, University of Groningen, Zernikelaan 25, 9747 AA Groningen, The Netherlands*

^b *Institute for Theoretical Physics, University of Utrecht, Utrecht, The Netherlands*

Abstract

We compare a relativistic covariant model for proton-proton bremsstrahlung with high-quality data from KVI. The agreement in large parts of phase space is satisfactory. However, remarkably large discrepancies are observed for specific kinematic regions. These failures are shown to occur primarily when the final two-nucleon system has energies less than about 15 MeV.

A. Introduction

The proton-proton bremsstrahlung ($pp\gamma$) process has attracted significant attention over the years, both experimentally and theoretically. In recent years, several new experiments have been performed [1–6], inspiring many new theoretical investigations [7–14]. In particular, a number of microscopic models have been developed to describe the $pp\gamma$ process. Examples are the potential model of Nakayama *et al.* [8] and the covariant model of Martinus *et al.* [10]. The theoretical predictions of these models could be compared to the $pp\gamma$ cross sections and analyzing powers for the TRIUMF experiment at 280 MeV [1]. The agreement of theory with these TRIUMF data is rather good, especially for the cross sections, provided that the experimental cross sections are renormalized [1]. Some outstanding discrepancies occur, however, for certain asymmetric proton angles.

More recently, the first high-precision data from the KVI experiment at 190 MeV became available [5], and many more data are forthcoming [6]. When comparing these data with theory, a pronounced and undisputable discrepancy between theory and experiment was observed in specific kinematic regions [5]. The size of the discrepancy between theory and experiment is disturbing, since what primarily enters are the two-nucleon (NN) interaction and the electromagnetic coupling of the photon to the NN system, both of which are believed to be accurately known at this energy. The high precision of the new KVI data allows one, in principle, to study smaller effects, like those arising from negative-energy states, the Δ -isobar, and meson-exchange currents. It is therefore important to identify the possible reasons for the discrepancies.

In this paper, we compare the covariant model of Ref. [10] with the KVI data available so far and analyze the discrepancies. We demonstrate that the dominant contribution to $pp\gamma$ for the specific problematic kinematic regions results when the NN interaction is evaluated at energies below about 15 MeV, and that, in fact, at least a major part of the problem resides in the low-energy behavior of the NN interaction models used.

This paper is organized as follows. First, we review briefly the covariant model for $pp\gamma$ and compare it to the KVI data in the problematic kinematic regions. Next, we demonstrate the sensitivity of the bremsstrahlung cross sections in these regions to the properties of the low-energy NN interaction. We then show that the problems can be significantly alleviated accordingly by improving the description of the interaction at low energies. We end by summarizing our conclusions.

B. Covariant model for bremsstrahlung

We first give a short review of the microscopic model of Martinus *et al.* for $pp\gamma$ [10]. In this covariant model the NN T -matrix is obtained by solving the Bethe-Salpeter equation for the two-nucleon system [15] in the equal-time approximation with the one-boson exchange (OBE) kernel of Ref. [16]. This OBE model for the NN interaction was, at that time, fitted to the Virginia Tech np partial-wave solution [17], by adjusting the meson-nucleon coupling constants and the form factor parameters, and a reasonable agreement was obtained.

This covariant NN T -matrix enters the model for $pp\gamma$, in which a number of contributions can be distinguished. The most important ones in the energy regime we consider here are the “nucleonic” contributions, consisting of single-scattering terms, *i.e.* photon emission

off the external proton legs (see Fig. 1, a-b), and the contribution commonly known as rescattering (see Fig. 1, c). The model is relativistic covariant and therefore negative-energy states are included in a natural way. The relevance of these negative-energy states is small for energies around 200 MeV. The reason [10] is that the contributions from the single-scattering diagrams where the intermediate nucleons are in a negative-energy state are canceled by similar contributions coming from the rescattering diagram. This cancellation holds for terms up to order $\mathcal{O}(q)$, where q is the photon momentum, and is a consequence of the soft-photon theorem [18].

Contributions from the Δ -isobar and from magnetic meson-exchange currents, containing in particular the $\omega\pi\gamma$ and $\rho\pi\gamma$ decay graphs, are also taken into account. These two-body current terms are included in a perturbative way, since they are small in general. The coupling constants of the photon to the various mesons were determined from the radiative decay widths of the vector mesons. As one can observe from Fig. 2 below, at an energy of 190 MeV the contribution of the two-body currents is small. These terms, however, increase in size with energy and can become appreciable around the pion-production threshold at 280 MeV and above.

This covariant bremsstrahlung model [10] is theoretically well founded and many of its ingredients have been tested in other calculations such as those for electron scattering on the deuteron [16]. Therefore, one did not expect *major* discrepancies with new experimental $pp\gamma$ data at energies below 280 MeV.

C. Comparison with the KVI data

In the KVI experiment, $pp\gamma$ cross sections and analyzing powers were measured for 190 MeV incoming proton energy, with the scattered protons detected at small forward angles, and with the photon emitted in the backward hemisphere [5]. A typical example of the KVI data [5] in comparison with theory is shown in Fig. 2. The data are plotted for two different kinematic situations, with θ_1 and θ_2 the fixed angles of the outgoing protons in the laboratory frame, and as function of the polar angle of emission of the photon, θ_γ . The theoretical predictions are from the model as published in Ref. [10].

For the asymmetric proton angles $\theta_1 = 8^\circ$, $\theta_2 = 16^\circ$ (upper left panel) the cross section shows a large discrepancy between theory and experiment for values of θ_γ corresponding to the backward peak in the cross section. For the symmetric proton angles $\theta_1 = \theta_2 = 16^\circ$ (upper right panel), on the other hand, the cross section shows a much better agreement between theory and data. The contribution of the two-body currents is seen to be minor, and thus the discrepancy for $\theta_1 = 8^\circ$, $\theta_2 = 16^\circ$ is unlikely to come from this source. In the following, we focus therefore on the nucleonic contribution as the cause of the problem.

Taking a closer look at the two kinematics presented in Fig. 2 reveals that the one which poses problems ($\theta_1 = 8^\circ$, $\theta_2 = 16^\circ$) is dominated by the contribution from the 1S_0 wave in the NN T -matrix, while for the second one for which the agreement is much better ($\theta_1 = \theta_2 = 16^\circ$) the 3P waves are as important as the 1S_0 wave. The contribution of the rescattering diagram is relatively small, suggesting that the problem resides already at the level of the single-scattering diagrams.

In the bremsstrahlung calculation the NN T -matrix is evaluated at different energies for each of the diagrams shown in Fig. 1. The energy is lowest for the diagrams where the

photon is emitted by one of the incoming protons. The value of this energy is shown in Fig. 3 as a function of θ_γ . For $\theta_1 = 8^\circ$, $\theta_2 = 16^\circ$, the T -matrix is evaluated at 7 and 11 MeV kinetic energy for the cases corresponding to the peaks in the bremsstrahlung cross sections, *i.e.* at about $\theta_\gamma = 20^\circ$ and 140° , respectively. For the minimum in the cross section, around $\theta_\gamma = 75^\circ$, the T -matrix is evaluated at 24 MeV when the photon is emitted by one of the incoming protons. In contrast, one observes that for $\theta_1 = \theta_2 = 16^\circ$, the T -matrix is evaluated at more than 20 MeV for $\theta_\gamma = 160^\circ$ and at more than 40 MeV for the minimum around $\theta_\gamma = 75^\circ$; see the upper panel of Fig. 3. Thus, we conclude that theory and experiment agree well for those situations where the T -matrix is evaluated above about 15 MeV, while the discrepancies occur for the cases corresponding to a lower energy.

In order to demonstrate the sensitivity of the $pp\gamma$ cross section to the low-energy NN interaction, we plot in the lower panel of Fig. 3 the cross section for $\theta_1 = 8^\circ$, $\theta_2 = 16^\circ$, where we only include the 1S_0 wave, for three values of the scattering length. Here we simply changed, for illustrative purpose only, the value of g_ε^2 , the coupling constant of the “ ε -meson” in the OBE model.

In Table 1 we list for the two cases, $\theta_1 = 8^\circ$, $\theta_2 = 16^\circ$ and $\theta_1 = \theta_2 = 16^\circ$, the cross sections calculated by including in the NN T -matrix only one of the important partial waves, *viz.* the 1S_0 wave and the 3P waves. This is done for the value of θ_γ corresponding to the backward peak or plateau in the cross section, *i.e.* $\theta_\gamma = 140^\circ$ in the first case and $\theta_\gamma = 160^\circ$ in the second case, respectively. In both cases the first number listed gives the cross sections with the T -matrix as used in Ref. [10] (the second number gives the corresponding value in the fit described below). It is seen that the contribution of the 1S_0 wave is significantly larger for the case $\theta_1 = 8^\circ$, $\theta_2 = 16^\circ$ compared to the case $\theta_1 = \theta_2 = 16^\circ$. By far the largest contribution to this 1S_0 cross section comes from radiation off the incoming proton legs. The 3P wave cross sections arise mainly from radiation off the outgoing proton legs. For $\theta_1 = 8^\circ$, $\theta_2 = 16^\circ$ emission from the incoming proton legs dominates the bremsstrahlung cross section, while for $\theta_1 = \theta_2 = 16^\circ$ emission from initial and final proton legs are comparable. The total cross sections listed in the bottom row of Table 1 include also the rescattering contribution.

At the time of its construction, the OBE model of Ref. [16] was fitted to the np phase-shift parameters of the Virginia Tech group, where the interest of the fit was at the higher energies. In view of our findings with the new high-precision $pp\gamma$ data, it becomes important to improve the description at low energies. In order to investigate whether at least the major part of the discrepancy between theory and the KVI data can be removed, we have performed a preliminary refit with an emphasis of obtaining better agreement with the Nijmegen pp partial-wave analysis of Ref. [19], at energies starting from 10 MeV up to 215 MeV.

In Fig. 4 we present the same calculation as in Fig. 2, but now for the NN model after the preliminary new fit. The description of the $pp\gamma$ cross sections in the region of the backward peak for $\theta_1 = 8^\circ$, $\theta_2 = 16^\circ$ has improved substantially. This is mainly due to the improvement in the description of the 1S_0 wave at low energies. Also the description of the 3P partial waves has improved. In Table 1 we now again list for the two kinematical situations the contribution to the $pp\gamma$ cross section of the different important partial waves. The new results should be compared to the values obtained with the model as published in Ref. [10], and also listed in Table 1.

A preliminary investigation suggests that for those regions in phase space where similar problems occurred as demonstrated here for the case $\theta_1 = 8^\circ$, $\theta_2 = 16^\circ$, at least a large part

of the problem is due to an inadequate description of the low-energy behavior of the NN T -matrix. Detailed results will be presented in Ref. [20].

Finally, it is worth pointing out that the sensitivity of the $pp\gamma$ cross sections to the low-energy NN interaction raises the question about the comparison between microscopic bremsstrahlung models of the type discussed here and soft-photon descriptions. The soft-photon amplitude of Ref. [11] gives a remarkably good description of the experimental $pp\gamma$ cross sections, including the data from KVI. In constructing the soft-photon amplitude, a specific choice is made for the on-shell points used in the calculation. For the kinematic situations discussed here, this choice does not correspond to the NN interaction at low energies, and therefore, the relation to microscopic models is not obvious.

D. Conclusions

In conclusion, the $pp\gamma$ cross section at 190 MeV varies strongly as a function of the angles of the protons. This can be traced back to an increasing contribution of the 1S_0 wave for the regions in phase space where the NN interaction is probed at low energies. For $\theta_1 = 8^\circ$, $\theta_2 = 16^\circ$, the 1S_0 wave dominates strongly at the peak of the cross section. In contrast, for $\theta_1 = \theta_2 = 16^\circ$, the 3P waves are as important as the 1S_0 wave.

The present study shows that the predicted cross sections in certain kinematic regions are sensitive to the NN interaction at low energy. In all cases, the analyzing powers are affected less by changes in the interaction. We have in particular not included in these calculations the Coulomb interaction, which plays an important role in the pp system at low energies. The results of such an analysis will be given in Ref. [20]. Only a limited set of KVI data has been published so far [5]. With the complete $pp\gamma$ data set [6], one may hope to be able to test in a quantitative way the validity of the various microscopic bremsstrahlung models.

Acknowledgments

We acknowledge discussions with our experimental colleagues at KVI. The research of R.G.E.T. was made possible by a fellowship of the Royal Netherlands Academy of Arts and Sciences. We thank M.C.M. Rentmeester for his help in setting up the codes for fitting the NN model.

REFERENCES

- [1] K. Michaelian *et al.*, Phys. Rev. D **41**, 2689 (1990).
- [2] R. Bilger *et al.*, Phys. Lett. B **429**, 195 (1998).
- [3] J. Zlomanczuk, A. Johansson, and the WASA-PROMICE Collaboration, Nucl. Phys. **A631**, 622c (1998).
- [4] K. Yasuda *et al.*, Phys. Rev. Lett. **82**, 4775 (1999).
- [5] N. Kalantar-Nayestanaki *et al.*, Nucl. Phys. **A631**, 242c (1998); H. Huisman *et al.*, Phys. Rev. Lett. **83**, 4017 (1999); Phys. Lett. B **476**, 9 (2000).
- [6] H. Huisman *et al.*, to be published.
- [7] V.R. Brown, P.L. Anthony, and J. Franklin, Phys. Rev. C **44**, 1296 (1991).
- [8] V. Herrmann and K. Nakayama, Phys. Rev. C **46**, 2199 (1992); F. de Jong *et al.*, Phys. Lett. B **333**, 1 (1994); F. de Jong, K. Nakayama, and T.S.H. Lee, Phys. Rev. C **51**, 2334 (1995); V. Herrmann *et al.*, Nucl. Phys. **A582**, 568 (1995).
- [9] J.A. Eden and M. Gari, Phys. Lett. B **347**, 187 (1995); Phys. Rev. C **53**, 1102 (1996).
- [10] G.H. Martinus, O. Scholten, and J.A. Tjon, Phys. Lett. B **402**, 7 (1997); Phys. Rev. C **56**, 2945 (1997); *ibid.* **58**, 686 (1998); Few Body Systems **26**, 197 (1999) G.H. Martinus, Ph.D. Thesis, University of Groningen, 1998.
- [11] M. K. Liou, R. Timmermans, and B. F. Gibson, Phys. Lett. B **345**, 372 (1995); *ibid.* **355**, 606(E) (1995); Phys. Rev. C **54**, 1574 (1996).
- [12] A.Yu. Korchin, and O. Scholten, Nucl. Phys. **A581**, 493 (1995); A.Yu. Korchin, O. Scholten, and D. Van Neck, Nucl. Phys. **A602**, 423 (1996).
- [13] Yi Li, M. K. Liou, R. Timmermans, and B. F. Gibson, Phys. Rev. C **58**, R1880 (1998).
- [14] S. Kondratyuk, G. Martinus, and O. Scholten, Phys. Lett. B **418**, 20 (1998).
- [15] J. Fleischer and J.A. Tjon, Nucl. Phys. **B84**, 375 (1974); Phys. Rev. D **15**, 2537 (1977); *ibid.* **21**, 87 (1990).
- [16] E. Hummel and J.A. Tjon, Phys. Rev. C **42**, 423 (1990); *ibid.* **49**, 21 (1994).
- [17] R.A. Arndt, J.S. Hyslop III, and L.D. Roper, Phys. Rev. D **35**, 128 (1987).
- [18] F.E. Low, Phys. Rev. **110**, 974 (1958).
- [19] V.G.J. Stoks *et al.*, Phys. Rev. C **48**, 792 (1993); M.C.M. Rentmeester *et al.*, Phys. Rev. Lett. **82**, 4992 (1999).
- [20] M.D. Cozma, O. Scholten, R.G.E. Timmermans, and J.A. Tjon, in preparation.

TABLES

	$\theta_1, \theta_2, \theta_\gamma = 8^\circ, 16^\circ, 140^\circ$		$\theta_1, \theta_2, \theta_\gamma = 16^\circ, 16^\circ, 160^\circ$	
1S_0	1.90	1.18	0.39	0.20
3P_0	0.02	0.02	0.01	0.02
3P_1	0.85	0.53	0.82	0.51
3P_2	0.43	0.42	0.53	0.47
initial	2.31	1.53	0.80	0.55
final	0.93	0.68	0.98	0.76
total	2.40	1.98	1.44	1.38

TABLE I. Cross sections, in $\mu\text{b}/\text{sr}^2\text{rad}$, for different kinematics $\theta_1, \theta_2, \theta_\gamma$, split up in partial waves, radiation from initial and final proton legs, and the total. For each kinematics, the first column gives the value of the original fit [10], while the second column gives the corresponding value after the refit.

FIGURES

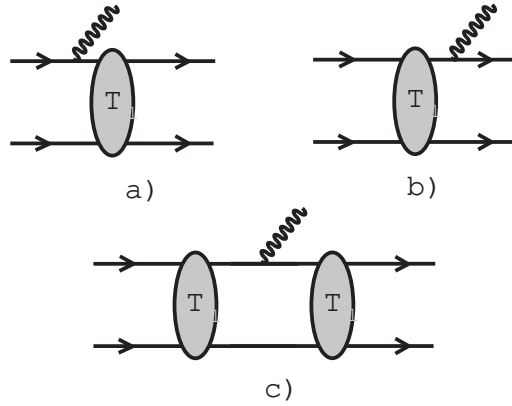


FIG. 1. Single scattering, a) and b), and rescattering, c), contributions to $pp\gamma$. Analogous diagrams in which the lower proton radiates the photon are not shown.

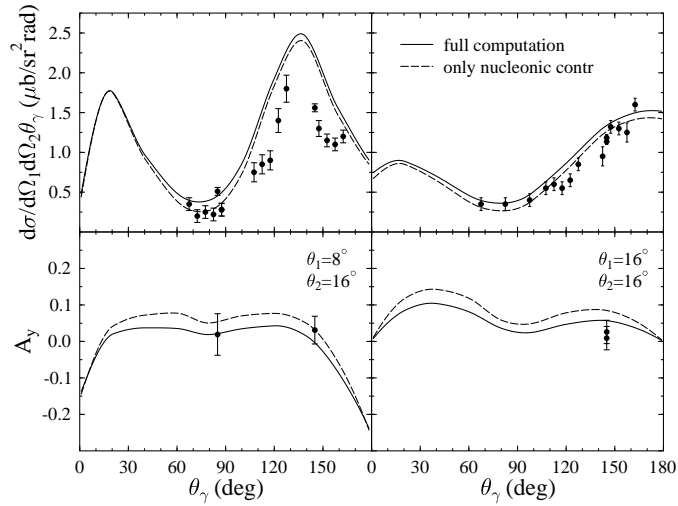


FIG. 2. Bremsstrahlung cross sections (upper panels) and analyzing powers (lower panels) at 190 MeV incoming proton energy, and for proton angles 8° , 16° (left panels) and 16° , 16° (right panels). The solid curves show the results of the full model, including negative-energy states and two-body currents, while the nucleonic contribution is shown by the dashed lines. The KVI data (partly preliminary) are taken from Refs. [5].

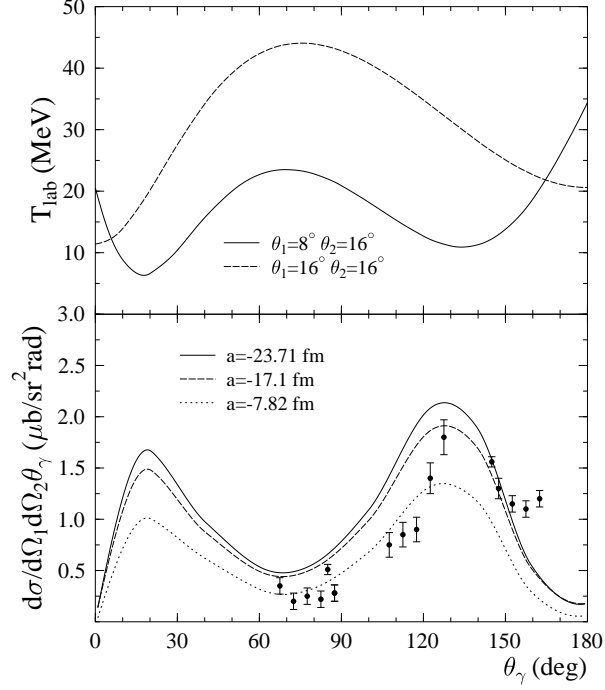


FIG. 3. Upper panel: kinetic energy of the incoming proton at which the NN T -matrix is evaluated for the two kinematics discussed in the text and in Fig. 2. Lower panel: bremsstrahlung cross sections at 190 MeV for three different scattering lengths for $\theta_1 = 8^\circ$, $\theta_2 = 16^\circ$. Only the contribution from the 1S_0 partial wave is included.

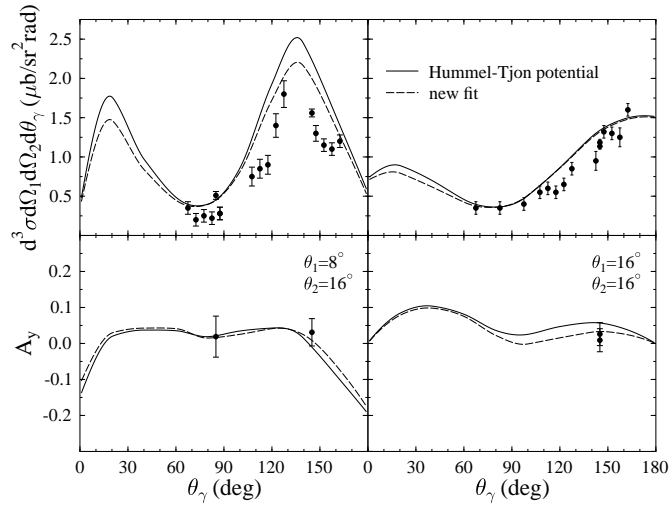


FIG. 4. Bremsstrahlung cross sections and analyzing powers at 190 MeV, for the same kinematics as in Fig. 2. The solid (dashed) curves show the results before (after) the refit of the NN model.